

SHEAR DEFORMABLE SHELL ELEMENTS FOR LARGE STRAINS AND ROTATIONS

M. BISCHOFF AND E. RAMM*

Institute of Structural Mechanics, University of Stuttgart, Germany

Dedicated to Eric Reissner, with our greatest respect for his scientific achievements

ABSTRACT

Well-known finite element concepts like the Assumed Natural Strain (ANS) and the Enhanced Assumed Strain (EAS) techniques are combined to derive efficient and reliable finite elements for continuum based shell formulations. In the present study two aspects are covered:

The first aspect focuses on the classical 5-parameter shell formulation with Reissner–Mindlin kinematics. The above-mentioned combinations, already discussed by Andelfinger and Ramm¹ for the linear case of a four-node shell element, are extended to geometrical non-linearities. In addition a nine-node quadrilateral variant is presented. A geometrically non-linear version of the EAS-approach is applied which is based on the enhancement of the Green–Lagrange strains instead of the displacement gradient as originally proposed by Simo and Armero.²

In the second part elements are derived in a similar way for a higher order, so-called 7-parameter non-linear shell formulation which includes the thickness stretch of the shell (Büchter and Ramm³). In order to avoid artificial stiffening caused by the three dimensional displacement field and termed ‘thickness locking’, special provisions for the thickness stretch have to be introduced. © 1997 John Wiley & Sons, Ltd.

Int. J. Numer. Meth. Engng., **40**, 4427–4449 (1997)

No. of Figures: 10. No. of Tables: 2. No. of References: 23.

KEY WORDS: element technology; geometrically non-linear shell formulation; enhanced assumed strains, higher order shell formulation; large strains; large rotations

1. SCOPE OF STUDY

The well-known phenomenon ‘locking’ of displacement based finite elements for thin-walled beams, plates and shells is caused by an unbalance of the trial functions. This unbalance, described in innumerable papers, can be cured by either reduction or enhancement of the degrees of freedom to tame the element-ansatz; or to use a more vivid explanation: Each static variable has to find its kinematic counterpart in an energy expression.

From the numerous remedies the following two have been proven to be, in particular, successful.

*Correspondence to: Ekkehard Ramm, Institut für Baustatik, Universität Stuttgart, Pfaffenwaldring 7, Postfach 1140, D-7000 Stuttgart 80, Germany

Contract grant sponsor: German National Science Foundation; Contract grant number: Ra218/7

- (1) The Assumed Natural Strain (ANS) Method: Here special interpolations for selected strain components are chosen to eliminate their parasitic influence. This objective is achieved evaluating the strains at the so-called 'sampling points' thus modifying the trials over the element domain. The ANS method has been proposed for plates by Hughes and Tezduyar⁴ to avoid shear locking and later on applied to shells by Dvorkin and Bathe.⁵ The procedure which is extremely simple and efficient is meanwhile a classical component of many element formulations and computer codes; it is also applied in this study.
- (2) The Enhanced Assumed Strain (EAS) Method: While the ANS method reduces the polynomial order of certain strain interpolations, the EAS method augments the strain field. Extra incompatible strain components are added to the conventional displacement-dependent compatible strains; consequently, their unbalanced components are adapted. The method has been originally proposed by Simo and Rifai⁶ and later on extended to large displacements by Simo and Armero.² Analogous to linear kinematics the displacement derivatives have been enhanced rather than the strains for the geometrically non-linear case.

Both schemes have a variationally sound basis. However, for the EAS method which has been derived from the three field variational principle of Hu–Washizu, it is not clear up to now what the role of the independent stress field is. There are strong indications that the EAS formulation is not a mixed method; but it is rather a displacement model with a limited softening effect. This also indicates that the stresses are to be derived by the conventional postprocessing step from the total enhanced strains via the constitutive law (Braess⁷).

One objective of the present study is a modified extension of the EAS method to geometrical non-linearities. Instead of a multiplicative decomposition of the deformation gradient as proposed by Simo and Armero² the Green–Lagrange strain tensor is additively decomposed into the compatible and the enhanced parts. This simplified version of the non-linear enhanced strains has already been described in Büchter and Ramm,³ see also Braun⁸ and Braun *et al.*⁹

It has already been mentioned that the shear locking in a 5-parameter formulation with Reissner–Mindlin kinematics may successfully be solved by the ANS method. However, the extension of the strain modification from the transverse shear also to inplane strains in order to avoid membrane locking and reduce mesh distortion sensitivity is not as successful. For the four node element, the reduction of the membrane strains is not sensible. Due to the Poisson effect the trials have to be at least bilinear. Efficient formulations for higher order elements are described in the literature (see, e.g. References 10 and 11). However, these elements do not satisfy the patchtest for constant strains and may exhibit poor performance in the case of distorted meshes.

Therefore in Andelfinger and Ramm¹ a combination of the ANS method for transverse shear and EAS extensions for inplane strains was proposed in the linear case for four-node elements. This concept is extended to geometrical non-linearities within the framework of arbitrarily large displacements and rotations in the present study. In addition to the four-noded element a new nine-node quadrilateral is presented.

The use of arbitrary three-dimensional constitutive equations without any modification was the driving force behind the higher order so-called 7-parameter formulation proposed in Büchter and Ramm³ and further elaborated in Büchter *et al.*¹² This 'extension into the three dimensions' covers also large strain problems and—most important—still keeps the basic and efficient shell assumption, namely the explicit integration across the thickness leading to stress resultants. The higher order kinematics is described by a linear variation of the thickness stretch which in turn counterbalances the linearly varying corresponding thickness stress.

The formulation has been extended to anisotropic laminated composite shells, see also Reference 9. In the present paper, the ANS and EAS combinations, applied already for the 5-parameter formulation, are also pursued for this 7-parameter model. However, due to the three-dimensional features of the theory, some arising problems have to be solved. In particular an extra artificial stiffening effect for curved structures, termed 'curvature thickness locking',¹³ has to be eliminated.

All extensions and modifications are underlined by several numerical examples. Alternative three-dimensional shell formulations have been presented by Parisch¹⁴ and Sansour.¹⁵ Verhoeven¹⁶ developed a plate theory including thickness stretch. These authors use a quadratic interpolation of the displacement across the thickness. Already earlier, Reissner¹⁷ derived a set of differential equations to treat finite axi-symmetrical deformations of shells including thickness strains.

2. AN ALTERNATIVE TO THE NON-LINEAR EAS FORMULATION

2.1. Variational basis

The extension of the EAS concept to geometrically non-linear problems by Simo and Armero² utilizes the enhancement of the displacement gradient and thus a multiplicative decomposition of the material deformation gradient \mathbf{F} . However, an alternative concept may be applied as well, see References 8, 12 and 18. Following the initial idea of the concept, the non-linear formulation may also be based on an additive decomposition of the Green–Lagrange strain tensor \mathbf{E} leading to similar equations as in the linear case. It will be shown that the present approach is very efficient and leads to practically the same numerical results for the investigated examples as the concept of Simo and Armero.

Although straightforward, the following considerations are important in connection with the variational consistency of the stress recovery. The variational formulation of the EAS method starts from the three field Hu–Washizu functional with the internal energy

$$\begin{aligned} \Pi(\mathbf{u}, \mathbf{E}, \mathbf{S}) = & \int_B W_s(\mathbf{E}) dV - \int_B \varrho \mathbf{b}^* \cdot \mathbf{u} dV + \int_B \mathbf{S} : (\tfrac{1}{2}(\mathbf{F}^T \mathbf{F} - \mathbf{g}) - \mathbf{E}) dV \\ & + \int_{\partial B_u} \mathbf{t} \cdot (\mathbf{u}^* - \mathbf{u}) dA - \int_{\partial B_\sigma} \mathbf{t}^* \cdot \mathbf{u} dA \end{aligned} \quad (1)$$

where \mathbf{F} is the deformation gradient depending on the displacement field \mathbf{u} , \mathbf{E} and \mathbf{S} are the Green–Lagrange strains and 2nd Kirchhoff–Piola stress tensors. \mathbf{g} is the metric tensor, ϱ the density, W_s the strain energy and \mathbf{t} the traction vector. The star (*) denotes prescribed values like the body force \mathbf{b}^* . All variables are referred to the initial configuration thus following a material formulation in the Lagrangean version.

The decisive step of the EAS method is the *reparametrization* of \mathbf{E} and its variation $\delta \mathbf{E}$, respectively:

$$\mathbf{E} = \mathbf{E}^u + \tilde{\mathbf{E}} \quad \text{with} \quad \mathbf{E}^u = \tfrac{1}{2}(\mathbf{F}^T \mathbf{F} - \mathbf{g}) \quad (2)$$

$$\delta \mathbf{E} = \delta \mathbf{E}^u + \delta \tilde{\mathbf{E}} \quad \text{with} \quad \delta \mathbf{E}^u = \mathbf{F}^T \delta \mathbf{F} \quad (3)$$

This means that the displacement-dependent compatible strains \mathbf{E}^u are enriched by a set of additional independent enhanced assumed strains $\tilde{\mathbf{E}}$. Introducing equations (2) and (3) into (1) yields

$$\begin{aligned}\tilde{\Pi}(\mathbf{u}, \tilde{\mathbf{E}}, \mathbf{S}) = & \int_B W_s(\mathbf{E}^u + \tilde{\mathbf{E}}) dV - \int_B \mathbf{q} \mathbf{b}^* \cdot \mathbf{u} dV - \int_B \mathbf{S} : \tilde{\mathbf{E}} dV \\ & + \int_{\partial B_u} \mathbf{t} \cdot (\mathbf{u}^* - \mathbf{u}) dA - \int_{\partial B_\sigma} \mathbf{t}^* \cdot \mathbf{u} dA\end{aligned}\quad (4)$$

Without loss of generality the boundary conditions for the displacements are omitted in the following expression. The variation of (4) leads to

$$\begin{aligned}\delta \tilde{\Pi}(\mathbf{u}, \tilde{\mathbf{E}}, \mathbf{S}) = & \int_B \left[\frac{\partial W_s}{\partial \mathbf{E}} : \delta \mathbf{E}^u + \frac{\partial W_s}{\partial \mathbf{E}} : \delta \tilde{\mathbf{E}} \right] dV - \int_B \mathbf{q} \mathbf{b}^* \cdot \delta \mathbf{u} dV \\ & - \int_B [\delta \mathbf{S} : \tilde{\mathbf{E}} + \mathbf{S} : \delta \tilde{\mathbf{E}}] dV - \int_{\partial B_\sigma} \mathbf{t}^* \cdot \delta \mathbf{u} dA\end{aligned}\quad (5)$$

The variation of the compatible strains, equation (3₂), is with $\delta \mathbf{F} = \text{Grad } \delta \mathbf{u}$

$$\delta \mathbf{E}^u = \mathbf{F}^T \text{Grad } \delta \mathbf{u} \quad (6)$$

The first expression in (5) can now be rewritten in terms of $\delta \mathbf{u}$

$$\frac{\partial W_s}{\partial \mathbf{E}} : \delta \mathbf{E}^u = \mathbf{F} \frac{\partial W_s}{\partial \mathbf{E}} : \text{Grad } \delta \mathbf{u} = \text{Div} \left(\mathbf{F} \frac{\partial W_s}{\partial \mathbf{E}} \delta \mathbf{u} \right) - \text{Div} \left(\mathbf{F} \frac{\partial W_s}{\partial \mathbf{E}} \right) \delta \mathbf{u} \quad (7)$$

With the help of the divergence theorem and $\delta \mathbf{u} = \mathbf{0}$ on ∂B_u

$$\int_B \text{Div} \left(\mathbf{F} \frac{\partial W_s}{\partial \mathbf{E}} \delta \mathbf{u} \right) dV = \int_{\partial B_\sigma} \left(\mathbf{F} \frac{\partial W_s}{\partial \mathbf{E}} \delta \mathbf{u} \right) \cdot \mathbf{n} dA \quad (8)$$

equation (5) is transformed into

$$\begin{aligned}\delta \tilde{\Pi}(\mathbf{u}, \tilde{\mathbf{E}}, \mathbf{S}) = & \int_B \left[- \text{Div} \left(\mathbf{F} \frac{\partial W_s}{\partial \mathbf{E}} \right) \cdot \delta \mathbf{u} + \frac{\partial W_s}{\partial \mathbf{E}} : \delta \tilde{\mathbf{E}} \right] dV - \int_B \mathbf{q} \mathbf{b}^* \cdot \delta \mathbf{u} dV \\ & - \int_B [\delta \mathbf{S} : \tilde{\mathbf{E}} + \mathbf{S} : \delta \tilde{\mathbf{E}}] dV - \int_{\partial B_\sigma} \left(\mathbf{t}^* - \mathbf{F} \frac{\partial W_s}{\partial \mathbf{E}} \cdot \mathbf{n} \right) \cdot \delta \mathbf{u} dA\end{aligned}\quad (9)$$

From this the weighted Euler equations in the domain can be derived

$$\begin{aligned}\int_B \delta \mathbf{u} \cdot \left[\text{Div} \left(\mathbf{F} \frac{\partial W_s}{\partial \mathbf{E}} \right) + \mathbf{q} \mathbf{b}^* \right] dV &= 0 \\ \int_B \delta \mathbf{S} : [\tilde{\mathbf{E}}] dV &= 0, \quad \int_B \delta \tilde{\mathbf{E}} : \left[\frac{\partial W_s}{\partial \mathbf{E}} - \mathbf{S} \right] dV = 0\end{aligned}\quad (10)$$

Since \mathbf{S} plays the role of a Lagrange parameter, whereas \mathbf{E} and \mathbf{u} are the primary variables, the saddle point solution renders a minimum for the latter and a maximum for \mathbf{S} . However, because

the stresses drop out of the formulation after discretization, the resulting finite elements are expected to follow the principle behaviour of a pure displacement model, i.e. $\Pi_h \leq \Pi$.

2.2. Discretization and linearization

Geometry and displacements are discretized by an isoparametric interpolation with nodal values \mathbf{x}_e and \mathbf{d} for co-ordinates and displacements, respectively. Enhanced strains and independent stresses are interpolated by functions \mathbf{M} and \mathbf{P} based on the parameters $\boldsymbol{\alpha}$ and $\boldsymbol{\beta}$, respectively. As usual h denotes the approximated fields

$$\begin{aligned}\mathbf{x} &\approx \mathbf{x}_h = \mathbf{N} \cdot \mathbf{x}_e; & \mathbf{u} &\approx \mathbf{u}_h = \mathbf{N} \cdot \mathbf{d} \\ \tilde{\mathbf{E}} &\approx \tilde{\mathbf{E}}_h = \mathbf{M} \cdot \boldsymbol{\alpha}; & \mathbf{S} &= \mathbf{S}_h = \mathbf{P} \cdot \boldsymbol{\beta}\end{aligned}\quad (11)$$

In order to reduce the three field functional $\tilde{\Pi}_h(\mathbf{u}_h, \tilde{\mathbf{E}}_h, \mathbf{S}_h)$ to a two field functional $\tilde{\tilde{\Pi}}(\mathbf{u}_h, \tilde{\mathbf{E}}_h)$ Simo and Rifai⁶ suggested to choose the interpolation of \mathbf{S}_h orthogonal to $\tilde{\mathbf{E}}_h$, i.e.

$$\int_B \mathbf{S}_h : \tilde{\mathbf{E}}_h dV = 0 \quad (12)$$

If the patchtest has to be satisfied the Jacobian needs to be at least constant in each element. If the orthogonality condition should hold for arbitrary stress and strain interpolations, equation (12) turns into

$$\int_{-1}^1 \int_{-1}^1 \mathbf{P}^T \mathbf{M} d\zeta d\eta = \mathbf{0} \quad (13)$$

The selection of feasible trial functions for the enhanced strain field according to equation (13) is a crucial point in this method. Furthermore, the enhanced strains have to be linearly independent of the compatible strains to avoid singular stiffness matrices. The consequences of these two conditions will be discussed in detail in the following sections.

Due to the orthogonality condition the third term of the discretized version of the functional (4) drops out

$$\tilde{\Pi}(\mathbf{u}, \tilde{\mathbf{E}}) \approx \tilde{\Pi}_h(\mathbf{d}, \boldsymbol{\alpha}) = \int_B W_s(\mathbf{E}_h^u(\mathbf{d}) + \tilde{\mathbf{E}}_h(\boldsymbol{\alpha})) dV - \Pi_h^{\text{ext}}(\mathbf{d}); \quad \Pi_h^{\text{ext}} = \mathbf{P}^* \cdot \mathbf{d} \quad (14)$$

It should be mentioned that for simplicity after discretization the same notation is kept although tensors now merge into vectors. \mathbf{P}^* is the vector of the nodal forces including body forces and other external loads.

Let us assume St. Venant–Kirchhoff material with the constant constitutive matrix \mathbf{C}

$$\tilde{\mathbf{S}}_h = \mathbf{C} \cdot \mathbf{E}_h \quad (15)$$

Note that in general $\hat{\mathbf{S}}_h$ is not identical with \mathbf{S}_h , i.e. $\hat{\mathbf{S}}$ satisfies the orthogonality condition only in the weak sense. In the past the variational significance of the stresses, obtained from strains through the constitutive law has been discussed, and orthogonalization procedures have been proposed.⁶ It can be seen from the Euler equations, that both \mathbf{S}_h and $\hat{\mathbf{S}}_h$ converge to the same values when the number of elements is increased to infinity.

The variation of (14) can be written as

$$\begin{aligned}\delta\tilde{\Pi}_h^{\text{int}}(\mathbf{d}, \boldsymbol{\alpha}) &= \delta\mathbf{d} \int_B (\mathbf{E}_{h,d}^u)^T \cdot \hat{\mathbf{S}}_h \, dV + \delta\boldsymbol{\alpha} \int_B (\tilde{\mathbf{E}}_{h,\alpha})^T \cdot \hat{\mathbf{S}}_h \, dV \\ \delta\Pi_h^{\text{ext}} &= \mathbf{P}^* \cdot \delta\mathbf{d}\end{aligned}\quad (16)$$

where the abbreviations $\delta\mathbf{E}_h^u = \partial\mathbf{E}_h^u/\partial\mathbf{d} \cdot \delta\mathbf{d} = \mathbf{E}_{h,d}^u \cdot \delta\mathbf{d}$ and $\delta\tilde{\mathbf{E}}_h = \partial\tilde{\mathbf{E}}_h/\partial\boldsymbol{\alpha} \cdot \delta\boldsymbol{\alpha} = \tilde{\mathbf{E}}_{h,\alpha} \cdot \delta\boldsymbol{\alpha}$ are introduced. Equation (16) is linearized by the directional derivatives with respect to the primary unknowns \mathbf{d} and $\boldsymbol{\alpha}$

$$\delta\tilde{\Pi}_h(\mathbf{d}, \boldsymbol{\alpha}) = \delta\tilde{\Pi}_h(\bar{\mathbf{d}}, \bar{\boldsymbol{\alpha}}) + \left. \frac{\partial\delta\tilde{\Pi}_h(\mathbf{d}, \boldsymbol{\alpha})}{\partial\mathbf{d}} \right|_{\mathbf{d}=\bar{\mathbf{d}}} \cdot \Delta\mathbf{d} + \left. \frac{\partial\delta\tilde{\Pi}_h(\mathbf{d}, \boldsymbol{\alpha})}{\partial\boldsymbol{\alpha}} \right|_{\boldsymbol{\alpha}=\bar{\boldsymbol{\alpha}}} \cdot \Delta\boldsymbol{\alpha} = 0 \quad (17)$$

with

$$\begin{aligned}\frac{\partial\delta\tilde{\Pi}_h(\mathbf{d}, \boldsymbol{\alpha})}{\partial\mathbf{d}} &= \delta\mathbf{d} \int_B [(\mathbf{E}_{h,dd}^u)^T \cdot \hat{\mathbf{S}}_h + (\mathbf{E}_{h,d}^u)^T \cdot \hat{\mathbf{S}}_{h,d}] \, dV + \delta\boldsymbol{\alpha} \int_B (\tilde{\mathbf{E}}_{h,\alpha})^T \cdot \hat{\mathbf{S}}_{h,d} \, dV \\ \frac{\partial\delta\tilde{\Pi}_h(\mathbf{d}, \boldsymbol{\alpha})}{\partial\boldsymbol{\alpha}} &= \delta\mathbf{d} \int_B (\mathbf{E}_{h,d}^u)^T \cdot \hat{\mathbf{S}}_{h,\alpha} \, dV + \delta\boldsymbol{\alpha} \int_B (\tilde{\mathbf{E}}_{h,\alpha})^T \cdot \hat{\mathbf{S}}_{h,\alpha} \, dV\end{aligned}$$

This leads to the linearized element matrix

$$\begin{bmatrix} \mathbf{K}_{e+u} + \mathbf{K}_g & \mathbf{L}^T \\ \mathbf{L} & \mathbf{D} \end{bmatrix} \cdot \begin{bmatrix} \Delta\mathbf{d} \\ \Delta\boldsymbol{\alpha} \end{bmatrix} = \begin{bmatrix} \mathbf{P}^* \\ \mathbf{0} \end{bmatrix} - \begin{bmatrix} \mathbf{R} \\ \tilde{\mathbf{R}} \end{bmatrix} \quad (18)$$

with the elastic/initial displacement and geometric stiffness matrix

$$\mathbf{K} = \mathbf{K}_{e+u} + \mathbf{K}_g$$

$$\mathbf{K}_{e+u} = \int_B (\mathbf{E}_{h,d}^u)^T \cdot \hat{\mathbf{S}}_{h,d} \, dV = \int_B \mathbf{B}^T \cdot \mathbf{C} \cdot \mathbf{B} \, dV; \quad \mathbf{K}_g = \int_B (\mathbf{E}_{h,dd}^u)^T \cdot \hat{\mathbf{S}}_h \, dV$$

coupling matrix

$$\mathbf{L} = \int_B (\tilde{\mathbf{E}}_{h,\alpha})^T \cdot \hat{\mathbf{S}}_{h,d} \, dV = \int_B \mathbf{M}^T \cdot \mathbf{C} \cdot \mathbf{B} \, dV$$

strain matrix

$$\mathbf{D} = \int_B (\tilde{\mathbf{E}}_{h,\alpha})^T \cdot \hat{\mathbf{S}}_{h,\alpha} \, dV = \int_B \mathbf{M}^T \cdot \mathbf{C} \cdot \mathbf{M} \, dV \quad (19)$$

and the internal force vectors

$$\begin{aligned}\mathbf{R} &= \int_B (\mathbf{E}_{h,d}^u)^T \cdot \hat{\mathbf{S}}_h \, dV = \int_B \mathbf{B}^T \cdot \hat{\mathbf{S}}_h \, dV \\ \tilde{\mathbf{R}} &= \int_B (\tilde{\mathbf{E}}_{h,\alpha})^T \cdot \hat{\mathbf{S}}_h \, dV = \int_B \mathbf{M}^T \cdot \hat{\mathbf{S}}_h \, dV\end{aligned}$$

Since the 'internal' strain parameters do not have to be compatible across the element boundaries they can be eliminated on the element level, leading to a modified stiffness expression for the EAS element

$$(\mathbf{K}_{e+u} + \mathbf{K}_g - \mathbf{L}^T \cdot \mathbf{D}^{-1} \cdot \mathbf{L}) \cdot \Delta \mathbf{d} = \mathbf{P}^* - \mathbf{R} + \mathbf{L}^T \cdot \mathbf{D}^{-1} \cdot \tilde{\mathbf{R}} \quad (20)$$

Again it can be recognized that the basic features of a displacement formulation are maintained. This characteristic makes the EAS method apparently more attractive for strain-driven material formulations like plasticity, than a conventional Hellinger–Reissner element formulation,¹⁹ based on stress and displacement interpolations.

Equation (20) also explains the reason for the extra numerical expense of the EAS formulation compared to other concepts, like the ANS method or reduced integration. In addition to the formation of the fully integrated stiffness matrix of a displacement element a second part has to be calculated, including a matrix inversion. However, it is apparent that this procedure only influences the computational time for the evaluation of the stiffness matrix.

Equation (20) is the basis for typical pathfollowing solution schemes, e.g. arc-length methods in connection with Newton–Raphson iterations.

Compared to the formulation of Simo and Armero² two advantages can be realized:

- (1) Only one additional expression \mathbf{K}_g in the tangential stiffness matrix has to be computed, compared to four in Reference 2.
- (2) Since non-linear terms do not result from the EAS extension, a 2×2 Gauss quadrature rule is sufficient for the integration of the enhanced strain terms, contrary to the original EAS formulation.

Compared to the non-linear EAS formulation proposed by Simo and Armero,² the implementation of the present concept is rather efficient because the extra terms do not enter the geometric stiffness matrix. Only the calculation of the residual forces $\tilde{\mathbf{R}}$ has to be added.

3. FIVE-PARAMETER SHELL FORMULATION

Shear deformable shell formulations with Reissner–Mindlin kinematics traditionally utilize 5 cross-sectional parameters to describe the deformation of the shell body, namely, 3 displacements of the shell midsurface plus two independent components of a rotation tensor. The director field can be interpolated without singularities using so-called Rodrigues parameters to update the director. A class of continuum based shell elements for small strains but large rotations of this kind has been described by Büchter and Ramm.²⁰ The 5-parameter shell elements discussed in the present study refer to the formulation therein.

3.1. Locking-free four-node shell elements

The four-node element described by Andelfinger and Ramm¹ for the linear case, can easily be extended to geometrical non-linearities. Here both, the ANS and the EAS extensions are applied to improve the poor performance of the original four-node displacement model.

The meanwhile 'classical' ANS approach to eliminate shear-locking effects due to Dvorkin and Bathe⁵ is also used herein. Thus the transverse shear strains of the displacement model are calculated at specially chosen sampling points and then interpolated within the element by linear-constant trial functions.

The membrane strains are enriched by the EAS method; here the essential point is a sensible choice of the extra enhanced strain modes. These have to be linearly independent from the compatible strains obtained by differentiating the displacement field.

The components of the linearized Green–Lagrange strain tensor for the in-plane strains of the shell are

$$E_{\alpha\beta} = \frac{1}{2}(u_{\alpha,\beta} + u_{\beta,\alpha}) = E_{\alpha\beta}^c + \theta^3 E_{\alpha\beta}^1, \quad \alpha, \beta \in \{1, 2\} \quad (21)$$

$E_{\alpha\beta}^c$ and $E_{\alpha\beta}^1$ are the membrane and the bending parts of the strains.

For a bilinear interpolation of the displacements

$$u_i \in \text{span} \{1, \xi, \eta, \xi\eta\} \quad (22)$$

the compatible membrane strains lead to

$$\begin{pmatrix} E_{11}^c \\ E_{22}^c \\ E_{12}^c \end{pmatrix} \in \text{span} \left[\begin{pmatrix} 1 \\ 0 \\ 0 \end{pmatrix} \begin{pmatrix} 0 \\ 1 \\ 0 \end{pmatrix} \begin{pmatrix} 0 \\ 0 \\ 1 \end{pmatrix} \begin{pmatrix} \eta \\ 0 \\ \xi \end{pmatrix} \begin{pmatrix} 0 \\ \xi \\ \eta \end{pmatrix} \right] \quad (23)$$

Therefore a maximum of seven bilinear enhanced strain components may be supplemented for a complete polynomial

$$\begin{pmatrix} \tilde{E}_{11}^c \\ \tilde{E}_{22}^c \\ \tilde{E}_{12}^c \end{pmatrix} \in \text{span} \left[\begin{pmatrix} \xi \\ 0 \\ 0 \end{pmatrix} \begin{pmatrix} 0 \\ \eta \\ 0 \end{pmatrix} \begin{pmatrix} 0 \\ 0 \\ \xi \end{pmatrix} \begin{pmatrix} 0 \\ 0 \\ \eta \end{pmatrix} \begin{pmatrix} \xi\eta \\ 0 \\ 0 \end{pmatrix} \begin{pmatrix} 0 \\ \xi\eta \\ 0 \end{pmatrix} \begin{pmatrix} 0 \\ 0 \\ \xi\eta \end{pmatrix} \right] \quad (24)$$

(1) (2) (3) (4) (5) (6) (7)

Further higher order terms are not meaningful.¹ The bending strains may be enhanced in the same way. However, compared to the additional numerical expense, the minor improvement of results does in general not justify this extension.

3.2. A note on the choice of enhanced strain interpolations

Recently, Andelfinger and Ramm¹ have pointed to the equivalence of hybrid stress elements based on the Hellinger–Reissner (HR) formulation and EAS elements, related to the Hu–Washizu variational principle. It has been stated that this equivalence holds if the trials for stresses in the HR elements are complementary to those for strains in the EAS approach.

As an example of the equivalence the EAS-7 membrane element and the hybrid-mixed element of Pian and Sumihara¹⁹ is mentioned.

A: Pian–Sumihara:

B: EAS-7:

Interpolations of stresses

Interpolations of strains

$$S^{11} = \beta^1 + \beta^4\eta$$

$$E_{11} = \alpha_1\xi + \alpha_5\xi\eta$$

$$S^{22} = \beta^2 + \beta^5\xi$$

$$E_{22} = \alpha_2\eta + \alpha_6\xi\eta$$

$$S^{12} = \beta^3$$

$$E_{12} = \alpha_3\xi + \alpha_4\eta + \alpha_7\xi\eta$$

(25)

β^1, \dots, β^5 and $\alpha_1, \dots, \alpha_7$ are the unknown parameters in the stress and strain trial, respectively. It is apparent that

- (1) No polynomial term in the stress interpolation in **A** shows up in its corresponding strain interpolation in **B**.
- (2) Stress and strain interpolation of **A** and **B** 'sum up' to a complete bilinear polynomial.

For the verification of the orthogonality condition (13) usually a constant stress distribution is assumed.^{6,1} This in turn leads to

$$\int_{-1}^1 \int_{-1}^1 \mathbf{M} d\xi d\eta = \mathbf{0} \quad (26)$$

However, the above-mentioned equivalence implies, that this assumption seems to be too strong. In fact it can easily be verified that the orthogonality condition also holds for the linear stress distribution of (25A). Therefore, it is anticipated that a variationally consistent stress field of an EAS element is complementing to the enhanced strain interpolation. Although not yet proven analytically this supposition will be confirmed below by numerical experiments.

3.3. A new nine-node quadrilateral

Analogous to the four-node element of Section 3.1 a nine-node shell element is derived. Again the ANS method is used to modify the transverse shear strain interpolation. The corresponding trial functions and the co-ordinates of the sampling points can be found, e.g. in Reference 10.

In Reference 10 also the membrane strains are modified by an ANS approach. However, the resulting element does not satisfy the patchtest for constant strains and exhibits poor performance for distorted meshes, especially in the case of nearly incompressible materials (see Figure 1).

In the present element—as in the four-node quadrilateral—the membrane strains are modified via the EAS method. The objectives of this procedure are as follows:

To obtain an element formulation, that is less sensitive to mesh distortions, variationally sound and that satisfies the patchtest;

To investigate, whether the equivalence of HR and EAS elements can be exploited to develop new element versions with reasonable enhanced strain interpolations.

To choose feasible trial functions for the enhanced strains the same considerations as for the four-node element are followed, see equations (23) and (24). The polynomial series of the compatible membrane strains is

$$\begin{pmatrix} E_{11}^c \\ E_{22}^c \\ E_{12}^c \end{pmatrix} \in \text{span} \left[\begin{pmatrix} 1 \\ 0 \\ 0 \end{pmatrix} \begin{pmatrix} 0 \\ 1 \\ 0 \end{pmatrix} \begin{pmatrix} 0 \\ 0 \\ 1 \end{pmatrix} \begin{pmatrix} \eta \\ 0 \\ \xi \end{pmatrix} \begin{pmatrix} 0 \\ \xi \\ \eta \end{pmatrix} \begin{pmatrix} \xi \\ 0 \\ 0 \end{pmatrix} \begin{pmatrix} 0 \\ \eta \\ \xi \end{pmatrix} \begin{pmatrix} 0 \\ 0 \\ \eta \end{pmatrix} \right] \quad (27)$$

$$\begin{pmatrix} \xi\eta \\ 0 \\ \xi^2 \end{pmatrix} \begin{pmatrix} 0 \\ \xi^2 \\ \xi\eta \end{pmatrix} \begin{pmatrix} \eta^2 \\ 0 \\ \xi\eta \end{pmatrix} \begin{pmatrix} 0 \\ \xi\eta \\ \eta^2 \end{pmatrix} \begin{pmatrix} \xi\eta^2 \\ 0 \\ \xi^2\eta \end{pmatrix} \begin{pmatrix} 0 \\ \xi^2\eta \\ \xi\eta^2 \end{pmatrix}$$

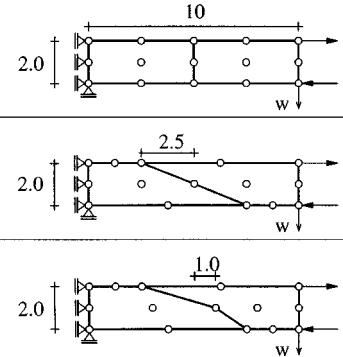
Cantilever beam, $\nu=0.4999$, plane strain		DISP	ANS (Pinsky)	EAS (present)
	$w =$	100%	100%	100%
	$w =$	100%	34.8%	100%
	$w =$	21.3%	63.2%	100.9%

Figure 1. Cantilever beam—effect of mesh distortion

For the choice of the enhanced strain interpolation we refer to the argumentation in Section 3.2. Firstly, the extra strains should be complementary to the assumed stresses. Secondly, no component in (27) is eligible for the enhancement, to ensure linear independence of \mathbf{E}^u and $\tilde{\mathbf{E}}$. For the stress assumptions, a balance has to be found between too few modes leading to spurious modes and too many components which render a stiffening solution.

The optimal choice for the nine-node element is:

A: Interpolations of stresses	B: Interpolations of strains
$S^{11} \in \text{span}(1, \xi, \eta, \xi\eta, \eta^2, \xi\eta^2)$	$E_{11} \in \text{span}(\xi^2, \xi^2\eta, \xi^2\eta^2)$
$S^{22} \in \text{span}(1, \xi, \eta, \xi\eta, \xi^2, \xi^2\eta)$	$E_{22} \in \text{span}(\eta^2, \xi\eta^2, \xi^2\eta^2)$
$S^{12} \in \text{span}(1, \xi, \eta, \xi\eta)$	$E_{12} \in \text{span}(\xi^2, \eta^2, \xi^2\eta, \xi\eta^2, \xi^2\eta^2)$

The stress interpolations (28A) have already successfully been used by Sansour 19 for the formulation of a hybrid-mixed nine-node element, based on the variational principle of Hellinger–Reissner. As in the case of the four-node element, the enhanced strain interpolations supplement the compatible strains to the order of the displacement interpolation (here: biquadratic).

It can be seen from (28), that this interpolation does apparently not satisfy the orthogonality condition. For example:

$$S^{11} = \beta_1; \quad E_{11} = \alpha_1 \cdot \xi^2 \rightarrow \int_{-1}^1 \int_{-1}^1 S^{11} \cdot E_{11} d\xi d\eta = \frac{4}{3} \beta_1 \cdot \alpha_1 \neq 0 \quad (29)$$

However, due to the mentioned equivalence theorem¹ it is anticipated that the method nevertheless works.

To overcome this apparent contradiction, the strain interpolations have to be slightly reformulated:

$E_{11} \in \text{span}(1 - 3\xi^2, \eta - 3\xi^2\eta, \eta^2 - 3\xi^2\eta^2)$
$E_{22} \in \text{span}(1 - 3\eta^2, \xi - 3\xi\eta^2, \xi^2 - 3\xi^2\eta^2)$
$E_{12} \in \text{span}(1 - 3\xi^2, 1 - 3\eta^2, \eta - 3\xi^2\eta, \xi - 3\xi\eta^2, 1 - 3(\xi^2 + \eta^2) + 9\xi^2\eta^2)$

In (30) the same polynomials are used as in (28). In addition, constant and linear terms are added, but due to their combination with the higher-order modes, they do not violate the condition of linear independence to the compatible strains. It can be easily verified that these trial functions ensure the orthogonality to the stresses (28A).

The advantage of this method is twofold:

- (1) The patchtest for constant and *linear* strains is satisfied.
- (2) The distortion sensitivity of the element is further reduced, even for the case of nearly incompressible materials. This fact is illustrated by a numerical example in Section 6.

The numerical effort for the calculation of the element stiffness matrix is definitely higher compared to the 'pure ANS' elements of Pinsky and Jang,¹⁶ i.e. from the efficiency point of view this element is in many cases inferior to other elements. However, the main advantage of the element is the fact that it is robust and free of any defects even for very thin shells, for geometrically linear and non-linear analysis, in the case of unstructured and highly distorted meshes and for almost incompressible materials.

In Figure 1 a simple two-element system is shown. The cantilever beam with end moment is often used to investigate the deformation sensitivity of bilinear elements. Here, three different nine-node elements are explored using an undistorted, a linearly distorted and a quadratically distorted mesh, respectively. Plane strain conditions and a nearly incompressible material make the results even more sensitive to mesh distortions.

The numerical results for the tip displacement w confirm the excellent behaviour of the proposed Enhanced Assumed Strain element compared to a pure displacement formulation and the Assumed Natural Strain element of Pinsky and Jang.¹⁰

4. SEVEN-PARAMETER SHELL FORMULATION

The shell formulation described in this section was first proposed by Büchter and Ramm.³ Notation and main aspects of the formulation are briefly repeated. For a more detailed description of the underlying concept see Büchter *et al.*¹² and Braun *et al.*⁷

4.1. Six-parameter formulation as basis

The extension of the classical 5-parameter shell formulation with Reissner–Mindlin kinematics is motivated by the following objective:

- (1) To handle large strain problems;
- (2) To use complete three-dimensional constitutive equations without any special treatment like the condensation of E_{33} ;
- (3) To extend the formulation to laminated and composite structures.

This can only be achieved by an additional degree of freedom which allows a thickness stretch of the shell. The resulting 6-parameter formulation maintains the full set of a completely three-dimensional stress and strain state.

4.2. Fundamental equations

The geometry and kinematic description of the shell body is illustrated in Figure 2. Values referring to the deformed configuration are denoted by a bar.

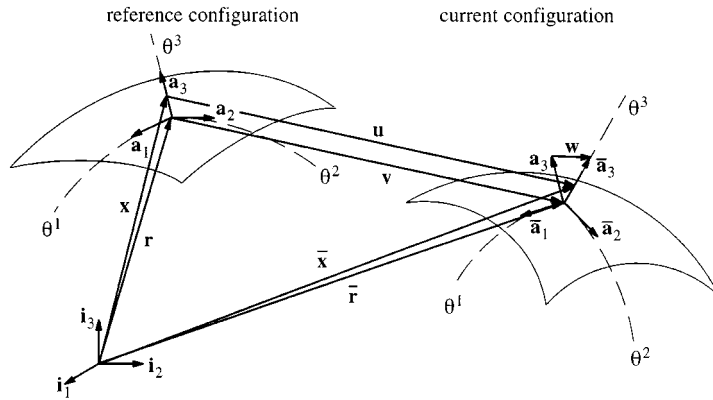


Figure 2. Geometry and kinematics of the shell

The midsurface of the shell is described by position vectors \mathbf{r} .

The covariant base vectors $\mathbf{a}_\alpha = \mathbf{r}_{,\alpha}$ define the metric of the shell at a given point of its midsurface, \mathbf{a}_3 is the *director* and defines the thickness direction of the shell. The position vector of an arbitrary point of the shell body and its metric vectors are given by

$$\mathbf{x} = \mathbf{r} + \theta^3 \mathbf{a}_3; \quad \mathbf{g}_\alpha = \mathbf{x}_{,\alpha} = \mathbf{a}_\alpha + \theta^3 \mathbf{a}_{3,\alpha}; \quad \mathbf{g}_3 = \mathbf{a}_3 \quad (31)$$

The displacement \mathbf{u} of a point of the shell body is composed of the displacement \mathbf{v} of the corresponding point on the midsurface and a difference vector \mathbf{w} :

$$\mathbf{u} = \bar{\mathbf{x}} - \mathbf{x} = \mathbf{v} + \theta^3 \mathbf{w}; \quad \mathbf{v} = \bar{\mathbf{r}} - \mathbf{r}; \quad \mathbf{w} = \bar{\mathbf{a}}_3 - \mathbf{a}_3 \quad (32)$$

Different from a conventional shell formulation with five independent degrees of freedom, in general, three displacements and two rotations, here the difference vector for the update of the director introduces a sixth displacement degree of freedom representing a thickness stretch of the shell.

It should be pointed out that this formulation reflects almost the same parametrization used for a brick element with two nodes on the upper and lower surface, except that the full set of 2×3 displacement parameters is replaced by the midsurface and the difference displacements; this improves the conditioning of the problem.

In terms of curvilinear co-ordinates (note that small Latin indices run from 1 to 3, Greek indices run from 1 to 2) the Green–Lagrange strain tensor is given by

$$\mathbf{E} = \frac{1}{2}(\bar{\mathbf{g}}_i \bar{\mathbf{g}}_j - \mathbf{g}_i \mathbf{g}_j) \mathbf{a}^i \otimes \mathbf{a}^j \quad (33)$$

with the covariant base vectors of the reference state \mathbf{g} and the deformed configuration $\bar{\mathbf{g}}$, respectively.

Neglecting the terms which are quadratic in θ^3

$$\mathbf{E} \approx \mathbf{E}^c + \theta^3 \mathbf{E}^l \quad \text{with} \quad \mathbf{E}^c = E_{ij}^c \mathbf{a}^i \otimes \mathbf{a}^j; \quad \mathbf{E}^l = E_{ij}^l \mathbf{a}^i \otimes \mathbf{a}^j \quad (34)$$

the covariant components of \mathbf{E} with respect to the metric tensor of the midsurface can be written as

$$\begin{aligned} E_{ij}^c &= \frac{1}{2}(\bar{\mathbf{a}}_i \bar{\mathbf{a}}_j - \mathbf{a}_i \mathbf{a}_j), & E_{\alpha 3}^l &= \frac{1}{2}(\bar{\mathbf{a}}_3 \bar{\mathbf{a}}_{3,\alpha} - \mathbf{a}_3 \mathbf{a}_{3,\alpha}) \\ E_{\alpha\beta}^l &= \frac{1}{2}(\bar{\mathbf{a}}_\alpha \bar{\mathbf{a}}_{\beta,3} + \bar{\mathbf{a}}_\beta \bar{\mathbf{a}}_{\alpha,3} - \mathbf{a}_\alpha \mathbf{a}_{\beta,3} - \mathbf{a}_\beta \mathbf{a}_{\alpha,3}), & E_{33}^l &= 0 \end{aligned} \quad (35)$$

4.3. Extension of transverse normal strains

The 6-parameter formulation has a severe deficiency in bending dominated cases with a non-vanishing Poisson's ratio ν . Due to the ν -coupling the transverse normal strains should also vary linearly across the thickness as the inplane normal strains. However, the linear displacement field in thickness direction results in a constant strain which in turn causes artificial stresses in thickness direction. This undesired stiffening effect is called 'Poisson Thickness Locking' (PTL) in the following.

It is essential to realize that—in contrast to a classical 'locking' effect—the resulting error does not diminish with mesh refinement. This is due to the fact that the origin of the stiffening lies in the formulation of the shell-theory, rather than in the formulation of the finite elements (Reference 9), or in other words: The discretization is usually not refined in thickness direction.

In order to remedy this defect, the displacement field across the thickness may be extended to a quadratic function (References 15 and 16).

$$u_1 = v_1 + \theta^3 \cdot w_1, \quad u_2 = v_2 + \theta^3 \cdot w_2, \quad u_3 = v_3 + \theta^3 \cdot w_3 + (\theta^3)^2 \cdot \bar{w}_3 \quad (36)$$

This formulation is free from the above-mentioned defect but now contains seven degrees of freedom per node. A possibility to remove the effect without increasing the number of degrees of freedom on the structural level has been proposed by Büchter and Ramm.³ The idea is to enrich the strain field of the element by an additional linear component \tilde{E}_{33}^1 of the thickness strain. This extra strain is introduced in the sense of a hybrid-mixed formulation, by the EAS method described in Section 2; for details see References 9 and 12.

According to the EAS concept the extra strain parameter \tilde{E}_{33}^1 is independently interpolated for each element, i.e. the additional parameters can be condensed out on the element level.

4.4. Interpolation of transverse normal strains

Extension of the transverse normal strain is now combined with the above-described modifications of membrane (EAS) and transverse shear (ANS) strains. Thus a four-node 7-parameter shell element is derived which is suited for thick as well as thin structures. However, one further problem still has to be overcome if coarse meshes and strong initial curvatures occur. This phenomenon termed 'Curvature Thickness Locking' (CTL) is explained in the following linear model problem.

An initially in-plane curved beam, including thickness stretch is discretized by linear displacement elements, as depicted in Figure 3. The vectors \mathbf{a}_3^z are the nodal directors of the beam elements. As in the shell formulation, the average of the directors is used at nodes between adjacent elements, where the discretized structure is only C^0 -continuous.

The beam is deformed due to a constant bending moment and the deformed geometry of one representative element is shown on the right-hand side of Figure 3. Analogous to the shell formulation, the rotation and deformation (thickness stretch) of the director is defined by a difference vector \mathbf{w} [see equation (32)]

$$\mathbf{u} = \mathbf{v} + \theta^3 \mathbf{w}; \quad \mathbf{u}_{,3} = \mathbf{w}; \quad \mathbf{g}_3 = \mathbf{a}_3 \quad (37)$$

From the linearized Green–Lagrange strain tensor

$$\mathbf{E} = \frac{1}{2}(\mathbf{g}_i \mathbf{u}_{,j} + \mathbf{g}_j \mathbf{u}_{,i}) \mathbf{g}^i \otimes \mathbf{g}^j \quad (38)$$



Figure 3. CTL-model problem: bending of an initially curved beam

the constant component of the normal strain in thickness direction can be obtained

$$E_{33} = \mathbf{g}_3 \cdot \mathbf{u}_{,3} \quad (39)$$

Together with (37), E_{33} can be written as

$$E_{33} = \mathbf{a}_3 \cdot \mathbf{w} \quad (40)$$

For a pure bending deformation and $\nu = 0$, it is expected that the length of the director is not changed during the deformation, i.e. \mathbf{w}^z has to be orthogonal to \mathbf{a}_3^z . It is now assumed that this condition holds at the nodal points, as indicated in the illustration of Figure 3. The director as well as the difference vector are interpolated linearly across the element domain

$$\begin{aligned} \mathbf{a}_3(\xi) &= \frac{1}{2}(1 - \xi) \cdot \mathbf{a}_3^1 + \frac{1}{2}(1 + \xi) \mathbf{a}_3^2 \\ \mathbf{w}(\xi) &= \frac{1}{2}(1 - \xi) \cdot \mathbf{w}^1 + \frac{1}{2}(1 + \xi) \mathbf{w}^2 \end{aligned} \quad (41)$$

The distribution of the transverse normal strain $E_{33}(\xi) = \mathbf{a}_3(\xi) \cdot \mathbf{w}(\xi)$ can be simplified if the orthogonality of \mathbf{a}_3^z and \mathbf{w}^z at the nodal points is taken into account

$$E_{33}(\xi) = \frac{1}{4} \left[(1 - \xi)^2 \cdot \underbrace{\mathbf{a}_3^1 \mathbf{w}^1}_{=0} + (1 - \xi^2) \cdot \mathbf{a}_3^1 \mathbf{w}^2 + (1 - \xi^2) \cdot \mathbf{a}_3^2 \mathbf{w}^1 + (1 + \xi)^2 \cdot \underbrace{\mathbf{a}_3^2 \mathbf{w}^2}_{=0} \right] \quad (42)$$

With the angle ϕ between the directors at the nodes 1 and 2 and $|\mathbf{w}| = e$, we finally get

$$E_{33}(\xi) = -\frac{1}{4}(1 - \xi^2) \cdot h \cdot e \sin \phi \quad (43)$$

where $h = 2 \cdot |\mathbf{a}_3^z|$ is the thickness of the beam. These ‘artificial thickness strains’ lead to additional terms in the internal energy of the element and therefore to a stiffening (locking).

From equation (43) it can be seen that

- (1) the physically correct strain $E_{33} = 0$ is obtained only for $\xi = \pm 1$, i.e. at the nodes of the element, if $\phi \neq 0$, i.e. for shells
- (2) $E_{33}(\xi) \equiv 0$, if the initial curvature is zero ($\phi = 0$), i.e. no problems arise for straight beams or plates, respectively;
- (3) the artificial strains depend on the angle of the directors in the undeformed configuration, therefore the locking effect is especially pronounced for coarse meshes and strong curvature;
- (4) in contrast to the artificial thickness strains described in Section 4.3 (PTL), in this case the stiffening effect diminishes with mesh refinement ($\phi \rightarrow 0$), so that the notion ‘locking’ seems to be more justified in this case;

The authors have already confronted these problems earlier and a possible remedy based on the ANS concept has been proposed in Ramm *et al.*¹³

The key feature of the parasitic strain distribution is the fact that they are zero at the nodes. Therefore, it suggests itself that an interpolation of the strains should be based on the *nodal* values instead of an evaluation at the *Gauss quadrature points*:

$$\hat{E}_{33}(\xi, \eta) = \sum_{K=1}^{NN} \tilde{N}^K(\xi, \eta) \cdot E_{33}(\xi^K, \eta^K) \quad (44)$$

This can be regarded as an ANS method with the nodes as sampling points. For the interpolation functions \tilde{N}^K the bilinear functions used for the displacements are the natural choice. The method has been presented in Reference 21; independently Betsch *et al.*¹⁸ developed the same idea. In Section 6 it will be shown that this modification is essential for a satisfactory element behaviour.

A similar effect can be observed for the nine-node element, even though not as strong. An interpolation according to (44) with quadratic interpolation functions noticeably improves the element behaviour.

4.5. A note on large strains

The handling of large strains in the framework of the present formulation follows the same procedure as for conventional brick elements. The 7-parameter shell formulation contains the complete set of a three-dimensional stress and strain state and any constitutive law can be applied without modification.

The feasibility of the shell formulation for large strain analysis has already been demonstrated by Büchter *et al.*,¹² and therefore it is not further set out in this paper. Since the present elements, despite several modifications, essentially result in a stiffness formulation, the advantages of the pure displacement models can be utilized.

Recently, Wriggers and Reese²² reported about a new kind of 'hourglassing' for EAS elements in geometrically non-linear analyses. The problem occurs in the case of large strain compression. This undesired instability also appears for the present non-linear EAS formulation, which is alternative to that in Wriggers and Reese.²² Both the four and the nine node element suffer from 'hourglassing' under certain strain states. Extra stabilizing methods seem to be necessary. It is interesting to note that the investigated example exhibits also a physical instability during loading.

5. SURVEY OF PROPOSED ELEMENTS

To sum up, one can say that the following strategies are followed to obtain an optimal element behaviour. Starting from an isoparametric displacement formulation of the four- and nine-node element, respectively, the following modifications are carried out for both the 5- and the 7-parameter shells:

- (i) The *membrane strains* are enriched with the help of the EAS method. In the case of the four-node element five additional parameters are used, 11 parameters are chosen to improve the nine-node element.
- (ii) For the *bending strains* the same procedure as for the membrane part (EAS) could be applied. However, due to the limited improvement, this concept is not recommended.

- (iii) For the improvement of the *transverse shear strains* the ANS method seems to be the best compromise between efficiency and numerical effort.

For the 7-parameter formulation additional modifications have to be taken into account:

- (1) The *linear part of the transverse shear strains* remains untouched. Its possible modification via the ANS method, analogous to its constant counterpart, proved to be of negligible influence.
- (2) The *constant part of the transverse normal strains* is modified with an ANS formulation. For the four-node element a bilinear interpolation is chosen, a biquadratic interpolation improves the behaviour of the nine-node element.
- (3) Finally, a *linear part of the transverse normal strains* is added by means of the EAS method.

6. NUMERICAL EXAMPLES

In this section the properties of the proposed elements are investigated for four benchmark problems, see Table I. For comparison the results of some established assumed strain elements (Bathe/Dvorkin, Pinsky/Jang) and the bicubic displacement element (16-DISP, 4×4 Gauss integration), are added. In Table II a survey of the applied elements is given.

A notation 9-E11/AT denotes a 9 node element with 11 extra EAS parameters (membrane strains), the ANS modification for the linear transverse shear strain and an ANS version for the thickness locking (CTL). GP denotes the number of integrations points applied within the Gauss quadrature.

It has already been mentioned that the numerical expense for the EAS formulation is not negligible. This is no surprise if it is taken into account that the calculation of the element stiffness matrix requires the inversion of strain matrix **D**. For example for the 9-E11/A element this is an 11×11 matrix.

To judge the efficiency of the proposed elements, numerical investigations have been carried out. Despite the computationally expensive calculation of the stiffness matrix, there is still a remarkable increase in quality, and therefore also in efficiency compared to displacement elements.

It is obvious that the numerical effort is less, if the ANS method rather than the EAS technique is applied. However, the authors are convinced that this shortcoming is at least balanced by the advantages of the EAS method: The patchtest is satisfied and the elements are less sensitive to mesh distortions.

6.1. Cook's membrane problem

In Section 2 a non-linear version of the EAS formulation has been presented which is in a way simpler than the version proposed by Simo and Armero². Therefore, a geometrically non-linear plane strain analysis of a trapezoidal membrane (see Figure 4) is carried out, applying the EAS formulation with multiplicative decomposition of the deformation gradient² and with additive decomposition of the strain tensor (*present*), respectively. The applied constitutive law is based on a non-linear elastic compressible Neo-Hooke formulation. Since the maximum strain level reached is about 5%, the application of a St. Venant-Kirchhoff description results only in slight deviations to the present solution.

Table I. Survey of numerical examples and its main objectives




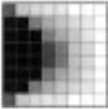
Plane Strain	5/7-Param. Shell	7-Param. Shell	Plane Stress
			
Cook's Membrane comparison of different non-linear EAS formulations	Pinched Hemisphere geometrical non-linearity, curvature thickness locking (CTL)	Scordelis-Lö Roof convergence of stresses	Plane Stress Problem stress recovery, equivalence of EAS and HR elements

Table II. Survey of investigated elements

5-parameter shell	$E_c^{z\beta}$	E_c^{z3}	—	—
4-A (Bathe/Dvorkin), 2×2 GP	DISP	ANS	—	—
4-E5/A (lin.: Andelfinger/Ramm), 2×2 GP	EAS-5	ANS	—	—
9-A/A (Pinsky/Jang), 3×3 GP	ANS	ANS	—	—
9-E11/A, 3×3 GP	EAS-11	ANS	—	—
16-DISP, 4×4 GP	DISP	DISP	—	—
7-parameter shell	$E_c^{z\beta}$	E_c^{z3}	E_c^{33}	E_1^{33}
4-E5/A, 2×2 GP	EAS-5	ANS	DISP	EAS
4-E5/AT,2×2 GP	EAS-5	ANS	ANS	EAS
9-E11/AT, 3×3 GP	EAS-11	ANS	ANS	EAS
16-DISP, 4×4 GP	DISP	DISP	DISP	EAS

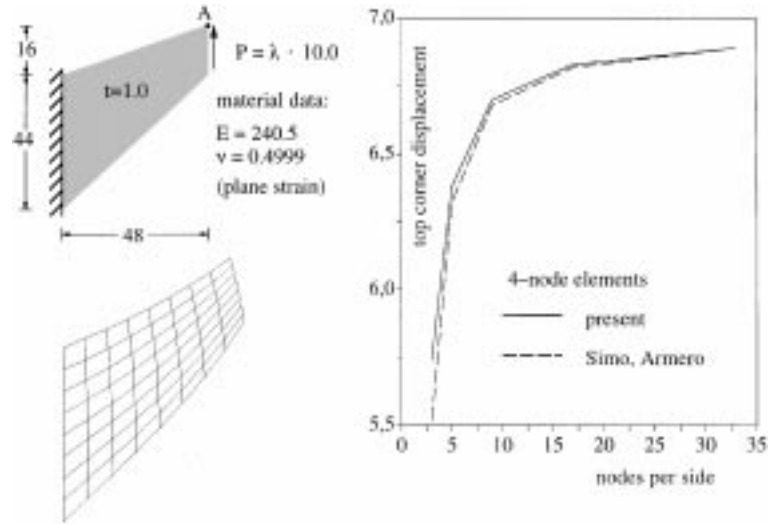


Figure 4. Cook's membrane, comparison of non-linear EAS formulations

The results obtained with either formulation are practically identical (Figure 4). It should be mentioned that the broken line results from measurements out of the diagram in Reference 2, and the reading error might be larger than the observed deviations.

6.2. *Pinched hemisphere with hole*

The hemisphere with hole is a common benchmark problem, both for geometrically linear and non-linear analyses. For the given, relatively slender, geometry of the shell, it is a small strain (at most 0.1 per cent) and large rotation problem.

It should be noted that due to the singularity of the displacements under concentrated loads, the absolute value of the displacement at point 'A' is not relevant. However, for the relative coarse meshes used herein the influence of this singularity is negligible,^{2,3} so that the results can be compared.

The example has been chosen to show the properties of the proposed non-linear EAS formulation and the resulting new shell elements. The 5-parameter formulation is applied, so the results can be compared to those obtained by other authors. Geometry and material data are given in Figure 5.

Figure 6 shows the results of the geometrically non-linear analysis. In both diagrams the solution obtained with 8×8 fully integrated 16-node displacement elements is added as a reference solution. The presented four-node element 4-E5/A appears to be more efficient than the pure ANS element 4-A of Bathe and Dvorkin. This has also been stated by Andelfinger and Ramm¹ for the geometrically linear case.

For the nine-node element the results are different. Here, the correspondence to the 'reference solution' is better for the ANS element of Pinsky and Jang 9-A/A than for the proposed EAS/ANS element 9-E11/A.

To demonstrate the importance of the modifications described in Section 4.4 (curvature thickness locking) a linear analysis, using the 7-parameter shell formulation is also carried out. Here the convergence properties of the 4-E5/A and 9-E11/A elements are compared to those of 4-E5/AT and 9-E11/AT (see Figure 7). It is obvious that the ANS modification of the transverse normal strains is essential for a satisfactory element behaviour. Even in the case of finer meshes there is a remarkable difference between the 4-E5/A and the 4-E5/AT element. As it was said already earlier, the effect is not that strong for the nine-node elements. But still the improvement of the results is obvious. The comparison to the 5 parameter solution illustrates the fact that the described modification fully eliminates the defect resulting from the parasitic thickness stretch.

6.3. *Scordelis-Lo roof*

Although there is a large number of publications on element technology, only few of them deal with the convergence of stresses. In most cases merely the displacements are taken into account when judging the quality of the proposed element. However, in most applications stresses are of primary interest. Therefore, a cylindrical shell, known as the 'Scordelis-Lo roof', subjected to dead load is chosen to investigate the convergence of the stresses (Figure 8). Again the 7-parameter shell formulation is applied. One quarter of the structure is discretized and a linear analysis is carried out.

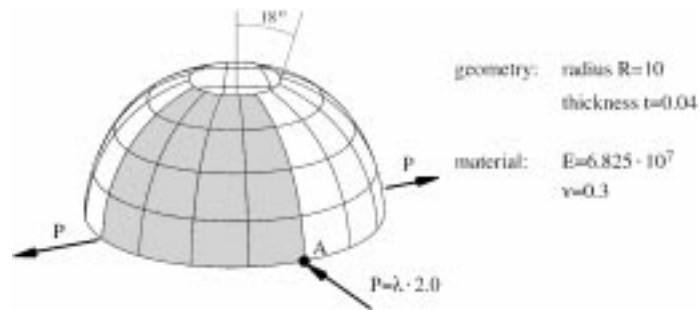


Figure 5. Pinched hemisphere under concentrated loads-5-parameter formulation

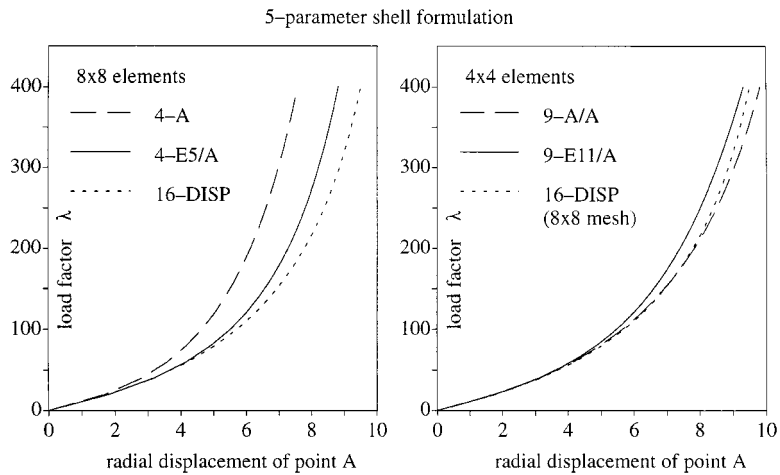


Figure 6. Pinched hemisphere—results

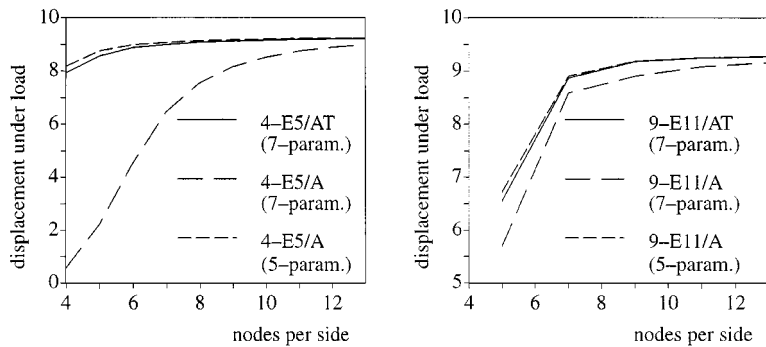


Figure 7. Pinched hemisphere—significance of CTL

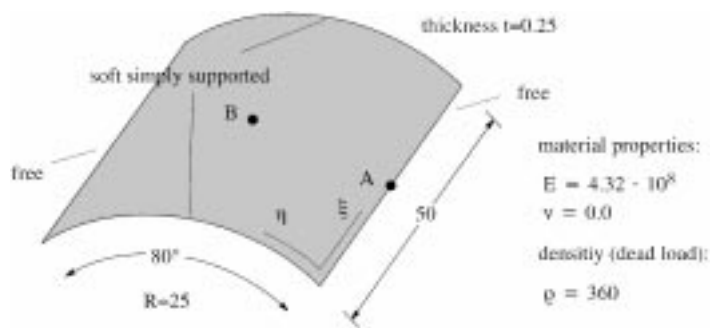


Figure 8. Scordelis-Lo roof: geometry and material data

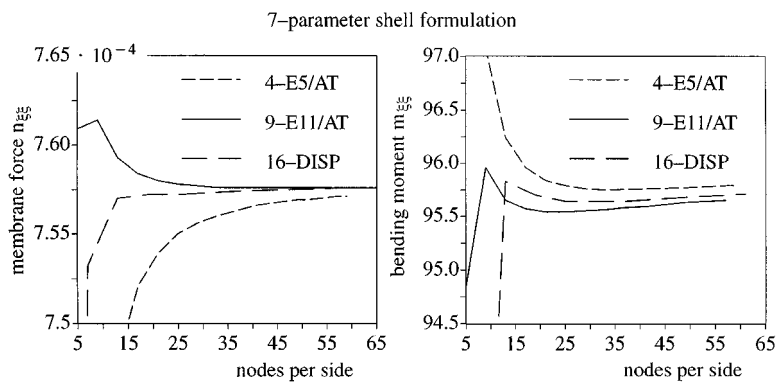


Figure 9. Scordelis-Lo roof: convergence of stresses

In the left diagram of Figure 9 the membrane force in the longitudinal direction of the cylinder at point A is plotted versus the number of nodes per side (quadratic element mesh). The element 9-E11/AT shows the best performance. The solution converges to the value of $7.5760 \cdot 10^{-4}$ already for 33 nodes per side which afterwards does not change anymore. Thus this value might be looked upon as the ‘exact’ (converged) solution. The 16-node displacement element converges to the same value, but not before 61 nodes per side are used. Finally, 4-E5/AT ends up at a deviation of 0.07 per cent for a discretization with 59 nodes per side.

Regarding the convergence of the bending moment $m_{\xi\xi}$ at point B in the middle of the shell, the situation is slightly different. Although the solution is relatively smooth in the investigated region no unique ‘converged solution’ (four significant digits) could be obtained with reasonable numerical effort. It can merely be recognized that the deviation for coarse meshes is again significantly smaller for the higher order elements.

6.4. Plane stress problem: stress recovery

In Section 3.2 the observed equivalence of hybrid-mixed elements based on the functional of Hellinger-Reissner and the EAS elements has been mentioned. The considerations concerning

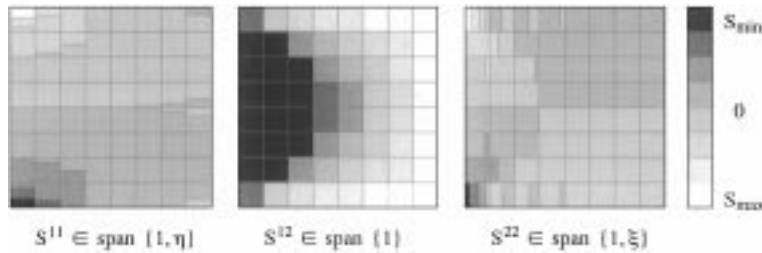


Figure 10. Plane stress problem, calculation of stresses

the optimal choice of feasible trial functions is valid both for the geometrically linear and non-linear range. So, if a new version of interpolation of the enhanced strains has to be tested only one subroutine has to be changed or supplemented to facilitate both linear and non-linear analyses. The formulation of the plane stress element of Pian and Sumihara¹⁵ and the EAS-7 membrane element¹ have been compared. Here 7 strain parameters are added to the 4-node displacement model.

To test this assumption, the stress distribution for a simple plane strain problem calculated with the EAS-7 element is shown in Figure 10. The plate is clamped on the left edge and subjected to dead load. Poisson's ratio has been chosen to be $\nu = 0.3$.

It can be seen from the contour lines (Figure 10) that the stress distributions perfectly correspond to the trials for the stresses in Reference 19 indicated in Figure 10, see also equation (25A). This is by no means self-evident, because the trials for the *strains* in the EAS-7 element are completely bilinear, see equations (23) and (25B).

This result not only confirms the equivalence of both elements but also indicates that the chosen stress recovery for the EAS element is variationally sound. However, the theoretical proof of the latter is still a matter of research and is hoped to be provided in the near future.

7. CONCLUSIONS

It has been shown that a non-linear version of the Enhanced Assumed Strain Method alternative to the one proposed by Simo and Armero² is possible, namely the additive decomposition of the Green–Lagrange strain tensor. The advantage of the concept is twofold:

- (1) Only one additional term (instead of four) has to be computed to form the geometrical stiffness matrix which in addition is independent of the EAS parameters.
- (2) A 2×2 Gauss quadrature is sufficient for the integration of the enhanced strain terms, contrary to the original EAS formulation. Furthermore, it is a straightforward extension to the linear EAS formulation and easy to code.

For the investigated example the results proved to be practically identical to those obtained by a multiplicative decomposition of the material deformation gradient. Both developed elements, a 4-node and a 9-node version, are applicable to shells with Reissner–Mindlin kinematics (5-parameter formulation) with arbitrarily large displacements and rotations and are free of locking. The extension to a fully three-dimensional version utilizing a so-called 7-parameter

formulation is capable to handle also large strain problems and non-modified three-dimensional constitutive laws. This extension into the three-dimensional stress and strain state usually causes a special kind of locking, termed 'curvature thickness locking'. This extra locking could also be overcome by an elegant and easy application of the ANS method.

As a by-product of the present formulation the formerly observed equivalence of mixed-hybrid elements, based on the Hellinger–Reissner functional and the EAS method, could be supported by further arguments.

ACKNOWLEDGEMENTS

The present study is supported by a grant of the German National Science Foundation (DFG, project Ra 218/7). This support is gratefully acknowledged. The authors would like to thank Dr.-Ing. Markus Braun who laid the foundation for the present study by his research on layered shells.

REFERENCES

1. U. Andelfinger and E. Ramm, 'EAS-elements for two-dimensional, three-dimensional, Plate and Shell structures and their Equivalence to HR-Elements', *Int. J. Numer. Meth. Engng.*, **36**, 1311–1337 (1993).
2. J. C. Simo and F. Armero, 'Geometrically non-linear enhanced strain mixed methods and the method of incompatible modes', *Int. J. Numer. Meth. Engng.*, **33**, 1413–1449 (1992).
3. N. Büchter and E. Ramm, '3D-extension of nonlinear shell equations based on the enhanced assumed strain concept', in Ch. Hirsch (ed.), *Computational Methods in Applied Sciences*, Elsevier, Amsterdam, 1992, pp. 55–62.
4. T. J. R. Hughes and T. E. Tezduyar, 'Finite elements based upon Mindlin plate theory with particular reference to the four-node isoparametric element', *J. Appl. Mech.*, **48**, 587–596 (1981).
5. E. N. Dvorkin and K. J. Bathe, 'A continuum mechanics based four-node shell element for general nonlinear analysis', *Engineering Comput.*, **1**, 77–88 (1984).
6. J. C. Simo and S. Rifai, 'A class of mixed assumed strain methods and the method of incompatible modes', *Int. J. Numer. Meth. Engng.*, **29**, 1595–1638 (1990).
7. D. Braess, 'Enhanced assumed strain elements and locking in membrane problems', submitted to *Comput. Meth. Appl. Mech. Engng.*, (1997).
8. M. Braun, Nichtlineare Analysen von geschichteten, elastischen Flächentragwerken, *Ph.D. Thesis*, Institut für Baustatik, Universität Stuttgart, 1994.
9. M. Braun, M. Bischoff and E. Ramm, 'Nonlinear shell formulations for complete three-dimensional constitutive laws including composites and laminates', *Comput. Mech.*, **15**, 1–18 (1994).
10. P. M. Pinsky and J. Jang, 'A C^0 -elastoplastic shell element based on assumed covariant strain interpolations', in G. N. Pande and J. Middleton (eds.), *Proc. Int. Conf. NUMETA 1987*, Swansea, 1987.
11. M. L. Bueale and K. J. Bathe, 'Higher-order MITC general shell elements', *Int. J. Numer. Meth. Engng.*, **36**, 3729–3754 (1993).
12. N. Büchter, E. Ramm and D. Roehl, 'Three-dimensional extension of nonlinear shell formulation based on the enhanced assumed strain concept', *Int. J. Numer. Meth. Engng.*, **37**, 2551–2568 (1994).
13. E. Ramm, M. Bischoff and M. Braun, 'Higher order nonlinear shell formulations—a step back into three dimensions', in K. Bell (ed.), *From Finite Elements to the Troll Platform*, Dept. of Structural Engineering, Norwegian Institute of Technology, Trondheim, Norway, 1994, pp. 65–88.
14. H. Parisch, 'A continuum-based shell theory for nonlinear applications', *Int. J. Numer. Meth. Engng.*, **38**, 1855–1883 (1993).
15. C. Sansour, 'A theory and finite element formulation of shells at finite deformations including thickness change: circumventing the use of a rotation tensor', *Arch. Appl. Mech.*, **10**, 194–216 (1995).
16. H. Verhoeven, Geometrisch und physikalisch nichtlineare finite Plattenelemente mit Berücksichtigung der Dickenverzerrung, *Ph.D. Thesis*, TU Berlin, Shaker, Aachen, 1993.
17. E. Reissner, 'On finite axis-symmetrical deformations of thin elastic shells of revolution', *Comput. Mech.*, **4**, 387–400 (1989).
18. P. Betsch, F. Gruttmann and E. Stein, 'A 4-node finite shell element for the implementation of general hyperelastic 3D-elasticity at finite strains', *Comput. Meth. Appl. Mech. Engng.*, **130**, 57–79 (1996).

19. T. H. H. Pian and K. Sumihara, 'A rational approach for assumed stress finite elements', *Int. J. Numer. Meth. Engng.*, **20**, 1685–1695 (1984).
20. N. Büchter and E. Ramm, 'Shell theory versus degeneration—a comparison in large rotation finite element analysis', *Int. J. Numer. Meth. Engng.*, **34**, 39–59 (1992).
21. M. Bischoff and E. Ramm, 'EAS methods for higher order nonlinear shell formulations', *3rd U.S. National Congress on Computational Mechanics (USNCCM)* at Dallas, Texas, 1995 (No proceedings).
22. P. Wriggers and S. Reese, 'An note on enhanced strain methods for large deformations', *Comput. Meth. Appl. Mech. Engng.*, **135**, 201–209 (1996).
23. T. Belytschko, 'A response to Babuska–Oden recommendations on benchmarks', *Int. Assoc. Comput. Mech. (IACM) Bull.*, **8**, 63–64 (1993).